

# Use of QUASES™/XPS measurements to determine the oxide composition and thickness on an iron substrate

A. P. Grosvenor,<sup>1,2\*</sup> B. A. Kobe,<sup>1</sup> N. S. McIntyre,<sup>1,2</sup> S. Tougaard<sup>3</sup> and W. N. Lennard<sup>4</sup>

<sup>1</sup> Surface Science Western, Room G-1, Western Science Centre, University of Western Ontario, London, Ontario N6A 5B7 Canada

<sup>2</sup> Department of Chemistry, University of Western Ontario, London, Ontario N6A 5B7 Canada

<sup>3</sup> Physics Institute, University of Southern Denmark, DK-5320 Odense, Denmark

<sup>4</sup> Department of Physics, University of Western Ontario, London, Ontario N6A 5B7, Canada

Received 20 January 2004; Revised 13 February 2004; Accepted 24 February 2004

QUASES™ Analyze and Generate were used to model the extrinsic loss structures for XPS spectra of oxide films grown on iron in such a way that their thickness and structure could be determined. The Generate program used in conjunction with spectra of model iron oxides allowed for both magnetite (Fe<sub>3</sub>O<sub>4</sub>) and maghaemite ( $\gamma$ -Fe<sub>2</sub>O<sub>3</sub>) structures to be identified in all films studied. These structures were identified as overlying layers in the oxide films and were usually intermixed at their interface. The absence of other iron oxide structures within the film could be tested based on their goodness of fit to the experimental spectrum. Comparison of the thickness values obtained using Generate with those found using nuclear reaction analysis suggested that the Generate results were higher by 20%. This difference likely resulted from the use of a calculated inelastic mean free path value for Fe 2p electrons in the Generate calculation rather than using the real attenuation length. For oxide films whose thickness approached 10 nm, the QUASES™ results for photoelectron spectra obtained with a Zr achromatic x-ray source were compared with those from the standard Al monochromatic source. In this particular case, the oxide thicknesses obtained using Generate and Analyze were found to be more consistent when the Zr source was used. Copyright © 2004 John Wiley & Sons, Ltd.

**KEYWORDS:** QUASES™; XPS; NRA; Fe oxidation

## INTRODUCTION

In the 1980s, Tougaard and co-workers<sup>1</sup> were able to demonstrate that the contributions of layered and/or laterally distributed surface phases could be calculated from the extrinsic background of an XPS spectrum. The Tougaard algorithms have been found to provide in-depth information to an approximate maximum depth of 5–10 $\lambda$  (IMFP, inelastic mean free path)<sup>2</sup> using loss structures extending as much as 200 eV in kinetic energy below the main photoelectron peak. Such algorithms were incorporated into a software package called QUASES™.<sup>3</sup>

Two different programs are included within the QUASES™ software package: the first program, 'Analyze', allows the user to model portions of the XPS spectral background using as variables the energy loss cross-section and the IMFP of the electron of interest. Although other cross-sections are available for use, the universal cross-section developed by Tougaard<sup>4</sup> is the most convenient for most materials. Apart from these variables, depth profile models such as "buried layer", "islands; passive substrate", "islands; active substrate", "exponential", and "several buried layers"

can be used with their resulting calculated extrinsic loss structure being compared with the experimental curve.

Also available with the QUASES™ software is the 'Generate' program, which allows for a model spectrum to be calculated using varying contributions of reference spectra along with the alterable parameters discussed above.<sup>5</sup> To date, most of the depth profiles analysed using QUASES™ have only been determined using the Analyze part of the software package,<sup>6–8</sup> with few authors using Generate.<sup>9</sup> This paper will demonstrate the usefulness of using both Generate and Analyze in combination to provide a more accurate picture of the near-surface oxide distribution of films grown on clean iron surfaces when exposed to oxygen. In particular, the Generate program has been used for the first time to identify and distinguish the distributions of two different iron oxide structures on the surfaces. The use of a higher energy Zr x-ray source coupled with QUASES™ analysis to quantify and identify oxides found in thick oxide films also will be described.

## EXPERIMENTAL

The surfaces of four polycrystalline Fe (99.995% pure) disks were polished to 0.5  $\mu$ m  $\gamma$ -Al<sub>2</sub>O<sub>3</sub> before being studied. After being placed in a vacuum, all four surfaces were sputter cleaned for 10 min using a 4 kV Ar<sup>+</sup> ion beam followed

\*Correspondence to: A. P. Grosvenor, Surface Science Western, Room G-1, Western Science Centre, University of Western Ontario, London, Ontario N6A 5B7, Canada. E-mail: agrosven@uwo.ca

by annealing at 600 °C for 30 min to reduce surface point defects. Following this, one sample was exposed to dry air (extra dry, Praxair), which was further dried using a silica-gel desiccant column, at atmospheric pressure and room temperature for 2 h before being placed back in a vacuum. The second sample was exposed to oxygen (medical grade, Praxair) at room temperature in a vacuum with a pressure of  $1.3 \times 10^{-2}$  Pa for 2 min before being analysed. Sample number three was exposed to air for 2 min before being placed back in a vacuum, and the fourth sample was exposed to air at 150 °C for 1 h before being analysed.

All XPS measurements were taken using a Kratos AXIS Ultra XPS spectrometer with Vision 2 acquisition software. Reference samples of metallic Fe,  $\alpha$ -Fe<sub>2</sub>O<sub>3</sub>,  $\gamma$ -Fe<sub>2</sub>O<sub>3</sub>, FeO and Fe<sub>3</sub>O<sub>4</sub> were prepared either under the cover of Ar gas or, for  $\alpha$ -Fe<sub>2</sub>O<sub>3</sub> and Fe<sub>3</sub>O<sub>4</sub>, in a vacuum so that new, fresh surfaces free of contamination were available. The Fe metal and powder samples (except for FeO) were obtained from Alfa Aesar (Ward Hill, MA). The sample of  $\alpha$ -Fe<sub>2</sub>O<sub>3</sub> (Boot Hill, NSW, Australia) was obtained from the Dana Mineral Collection found at the Department of Earth Sciences, University of Western Ontario. The Fe<sub>3</sub>O<sub>4</sub> sample (Mesabi Range, MN) was obtained from a mineral collection owned by Ross Davidson. FeO was prepared by reducing  $\alpha$ -Fe<sub>2</sub>O<sub>3</sub> in flowing hydrogen gas at 600 °C.<sup>10</sup>

While collecting the survey scans of the different samples, the following parameters were used: Al K $\alpha$  excitation source, electron take-off angle = 90°, energy range = 1100–0 eV, pass energy = 160 eV, step size = 0.7 eV, sweep time = 180 s and x-ray spot size = 700 × 400  $\mu$ m. To confirm the oxidation state of the various Fe species, high-resolution scans were also taken using a pass energy of 40 eV. The energy resolution at this pass energy for high-resolution spectra found using

the Al K $\alpha$  x-ray source is 0.6 eV. All energy scales from the high-resolution spectra were adjusted to give a C 1s value of 285 eV. For samples three and four, survey spectra of their surfaces were also taken using the achromatic Zr L x-ray source found on the Kratos XPS.

## QUASES™

### 'Analyze'

To determine the approximate oxide layer depth, QUASES™ Analyze was used to assess the oxide thickness from the O 1s extrinsic loss structure. Also, the overlayer thickness attributed to contamination from carbon was determined using the Fe 2p spectrum. The IMFP values used during this analysis were calculated using the Tougaard TPP-2M calculator provided with the QUASES™ software package. The calculator, which can be freely downloaded from [www.quases.com](http://www.quases.com), uses the TPP-2M formula due to Tanuma *et al.*<sup>11</sup> The values for O 1s and Fe 2p were determined using Fe<sub>3</sub>O<sub>4</sub> as the model compound and kinetic energies of 956 eV (O 1s) and 775 eV (Fe 2p<sub>3/2</sub>).

### 'Generate'

Generate was used to determine the depth of individual oxide layers using only the Fe 2p region. Spectra from the reference compounds discussed above were all used either separately or in combination to model the experimental spectra under consideration. The surfaces were always modelled in such a way that the Fe<sup>(0)</sup> metal spectra remained as the bulk (unless otherwise stated), with the Fe<sup>2+</sup> compounds coming next, followed by the Fe<sup>3+</sup> compounds (if required) that were closest to the surface. A spectrum was deemed to have been adequately fit if the model spectra almost or completely overlaid the extrinsic background

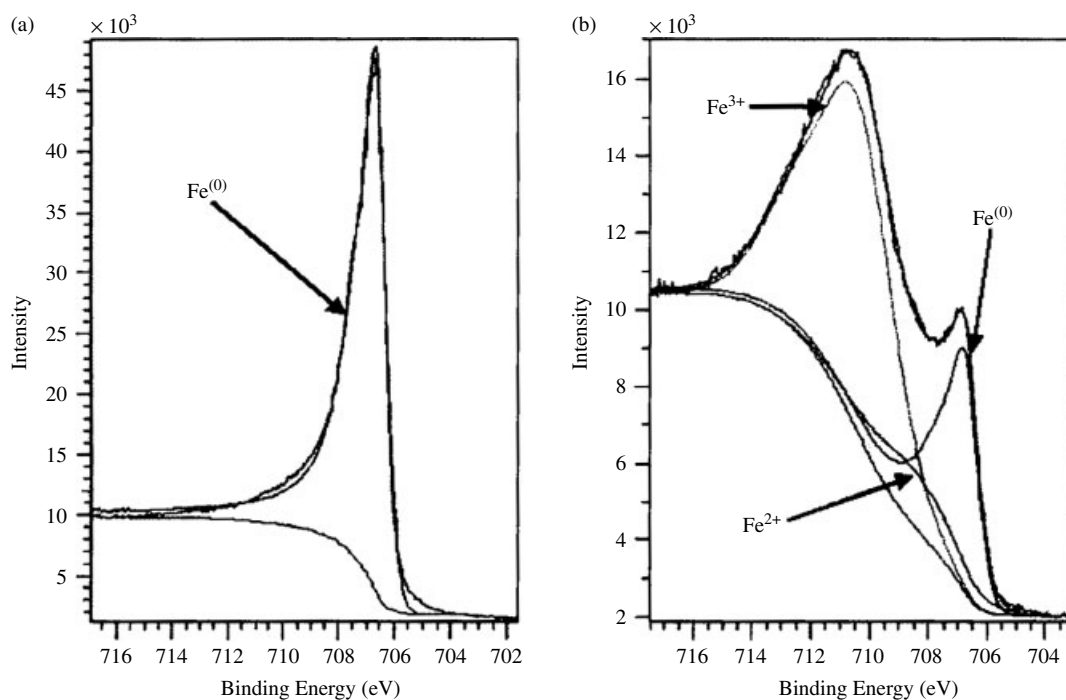


**Figure 1.** High-resolution spectra of the 2p<sub>3/2</sub> photoelectron peak from a clean Fe metal surface (a) and an Fe surface dry-air-oxidized for 2 h (b). A Shirley-type background was used during the fitting of both high-resolution spectra.

region of the experimental spectra located between 720 and 750 eV (kinetic energy). Only those spectra with films that started and ended before the overall thickness reached  $6-7\lambda$  were used. This range was chosen based on previous research done in this laboratory as well as that performed by Tougaard.<sup>2</sup>

### Strohmeier overlayer equation

As a comparison to the usual methods of determining the oxide depth found on surfaces by XPS, the QUASES™-determined results were compared to angle-resolved XPS (ARXPS) data found for the same sample. To determine the oxide depth  $d$  the following equation was used<sup>12</sup>

$$d = \lambda_0 \sin \Theta \ln \left( \frac{N_m \lambda_m I_o}{N_o \lambda_o I_m} + 1 \right).$$

where subscripts  $O$  and  $m$  stand for oxide and metal,  $\theta$  represents the electron take-off angle used,  $N$  represents the volume density of metal atoms in either the metal or oxide,  $\lambda$  represents the IMFP that accounts for energy loss due to inelastic electron scattering and  $I$  represents the intensity (peak area) of either the metal or oxide Fe 2p<sub>3/2</sub> photoelectron peaks.<sup>11</sup> The maximum depth probed using this method is believed to be  $\sim 10$  nm,<sup>12</sup> making it comparable in this respect to the Tougaard method.

### Nuclear reaction analysis

To determine the atom density of oxygen in the oxide film, nuclear reaction analysis (NRA) was used. A 2.5 MV Van de Graaff accelerator using a deuterium ion beam and a silicon-charged particle detector was used to oversee the

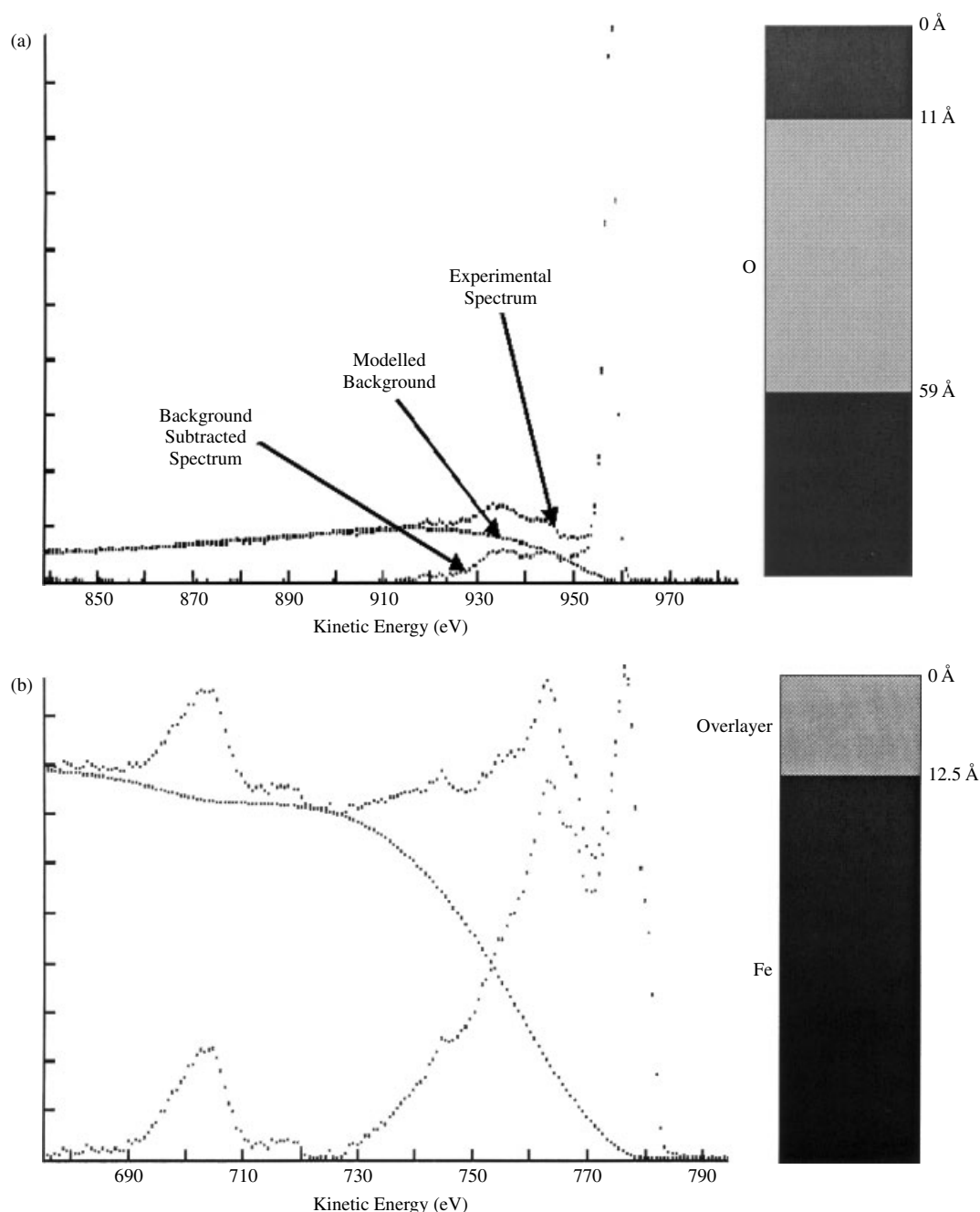


**Figure 2.** QUASES™ Analyze-modelled peaks from an Fe surface after exposure to dry air for 2 h: (a) O 1s; (b) Fe 2p.

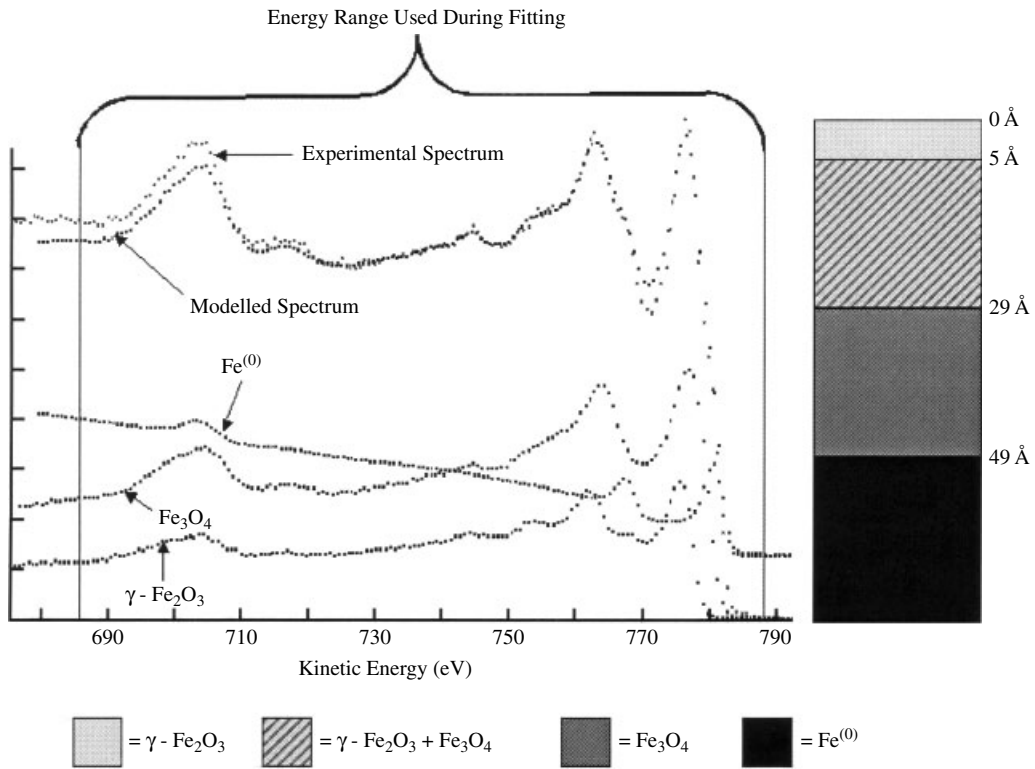


**Figure 3.** Results found using QUASES™ Generate with spectra of  $\gamma$ -Fe<sub>2</sub>O<sub>3</sub> and Fe<sub>3</sub>O<sub>4</sub> acting as the references. The experimental spectrum represents the Fe 2p XPS signal after exposure of a clean Fe surface to dry air for 2 h. The overlayer thickness was determined from the Analyze results of the Fe 2p portion of the spectra. The model spectrum used for  $\gamma$ -Fe<sub>2</sub>O<sub>3</sub> was shifted upwards by 2.0 eV and the spectrum used for Fe<sup>(0)</sup> was shifted upwards by 0.5 eV for best fit. The requirements of energy shifts were probably the result of charging of the oxides when their reference spectra were taken.

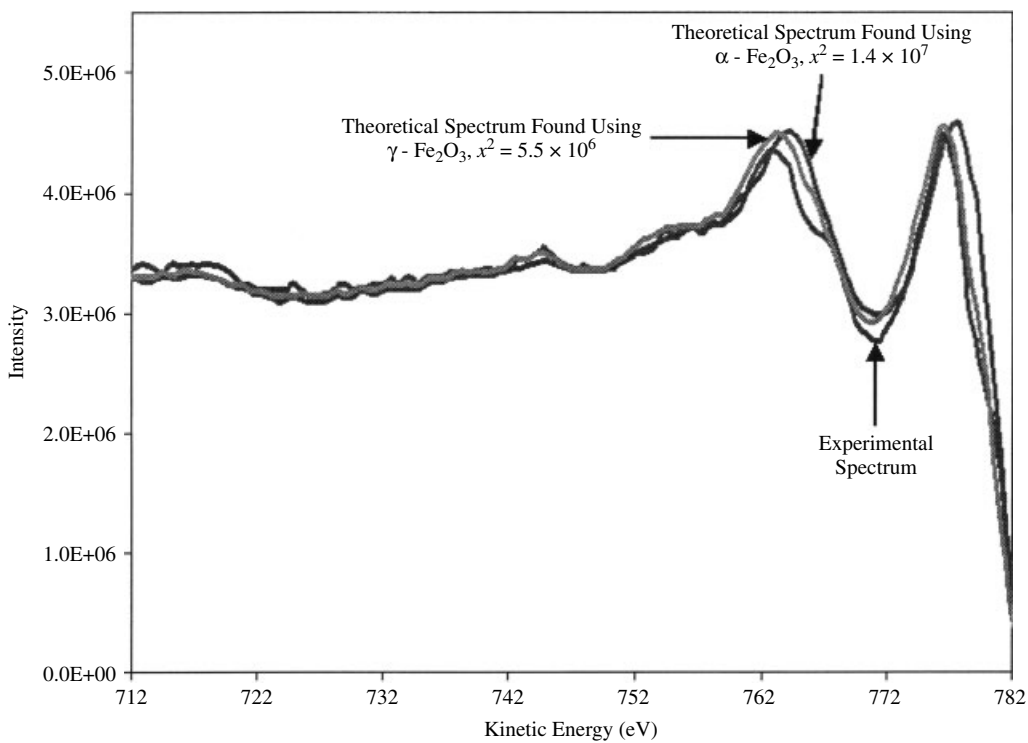


**Figure 4.** Graph of the experimental and theoretically modelled Fe 2p results discussed above for the Fe surface exposed to dry air for 2 h, along with their chi-squared values, indicating the modelled spectra's goodness of fit. Both the  $\gamma$ - and  $\alpha$ -Fe<sub>2</sub>O<sub>3</sub> spectra were shifted upwards by 2 eV to achieve the best fit.

following nuclear reaction:  $^{16}\text{O}(\text{d}, \text{p})^{17}\text{O}$ . The oxide thickness was calculated after relating the results to the oxygen density from a sample of  $\text{Ta}_2\text{O}_5$  with a known thickness ( $707 \text{ \AA} \pm 2\%$ ).

## RESULTS

### Aluminium $K\alpha$ x-ray source

Figure 1 compares the Fe  $2\text{p}_{3/2}$  spectra found for the clean Fe surface (Fig. 1(a)) and for the surface following its exposure to dry air for 2 h at room temperature (Fig. 1(b)). After accounting for the metallic contribution to the spectrum in Fig. 1(b), both  $\text{Fe}^{2+}$  and  $\text{Fe}^{3+}$  contributions could be roughly distinguished based on model spectra of  $\text{Fe}_3\text{O}_4$ , FeO and  $\alpha\text{-Fe}_2\text{O}_3$ .

The oxidized surface was modelled first using QUASES<sup>TM</sup> Analyze, where an approximate oxide thickness of 4.8 nm was found based on fitting the O 1s peak after removing the extrinsic energy loss background. Analysis of the Fe 2p spectrum also indicated that the Fe component began at 1.25 nm below the surface; these results would suggest that the top portion of the surface must contain species such as carbon, adsorbed water and other impurities. Figure 2 shows the two modelled spectra discussed above, with diagrams of the surfaces indicating both the starting and ending depths.

After the general profile was determined, QUASES<sup>TM</sup> Generate was used to identify the type of oxides found in the oxide layer. At room temperature and pressure, previous research has indicated that FeO will form first but because it is unstable at temperatures below  $570^\circ\text{C}$  it is

quickly transformed into  $\text{Fe}_3\text{O}_4$  with an  $\text{Fe}_2\text{O}_3$  overlayer.<sup>13</sup> It has been found also that when Fe is oxidized in a dry atmosphere  $\gamma\text{-Fe}_2\text{O}_3$  is formed rather than  $\alpha\text{-Fe}_2\text{O}_3$ .<sup>14a</sup> Spectra from both  $\text{Fe}_3\text{O}_4$  and  $\gamma\text{-Fe}_2\text{O}_3$  with varying layer thicknesses on Fe metal were used to model the surface oxide layer, with the results shown in Fig. 3. Inspection of Fig. 3 will show the distinctive differences between the features in the extrinsic loss spectral portions for  $\text{Fe}_3\text{O}_4$  and  $\gamma\text{-Fe}_2\text{O}_3$  as well as differences in the slopes of the spectra. The slope and structure of the extrinsic loss spectrum for Fe metal are distinguishable from those of the oxides. To achieve the best fit to the experimental spectrum, the reference spectra from  $\gamma\text{-Fe}_2\text{O}_3$  and  $\text{Fe}^{(0)}$  were shifted upwards by 2.0 eV and 0.5 eV (kinetic energy scale), respectively. The requirement of energy shifts was probably the result of charging of the oxides when their reference spectra were taken.

The extrinsic background located between  $\sim 720$  eV and 750 eV was particularly well fit. The portion of the spectra located just above the photoelectron peaks using the kinetic energy scale was not well modelled owing to the preponderance of intrinsic electrons in this range. The oxide/metal interface depth found was close to that obtained by QUASES<sup>TM</sup> Analyze. The model indicates that rather than there being fixed interfaces between the different oxides, which has been proposed by other authors,<sup>14b,15</sup> the oxide layers actually appeared to be mixed into each other.

An absolute measure of the quantity of oxygen on this surface was obtained using NRA. This same technique has been used previously to calibrate the oxide thickness

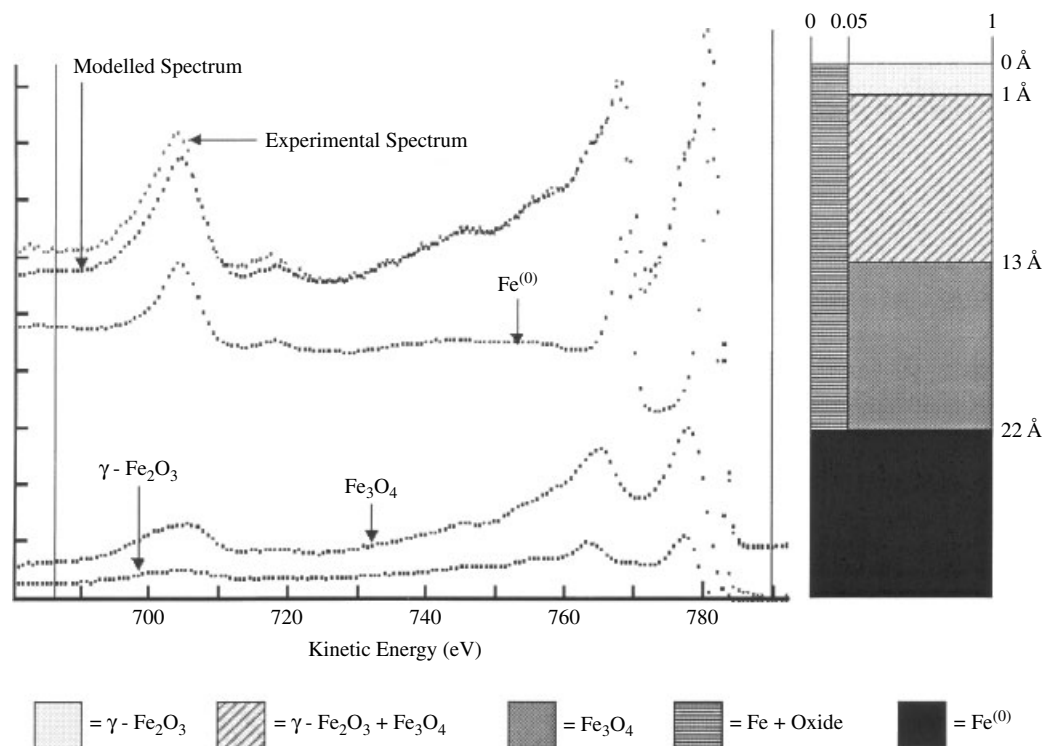


**Figure 5.** Results found using QUASES<sup>TM</sup> Generate with Fe 2p spectra of  $\gamma\text{-Fe}_2\text{O}_3$ ,  $\text{Fe}_3\text{O}_4$  and Fe metal acting as the references for an Fe surface exposed to oxygen at  $1.3 \times 10^{-2}$  Pa for 2 min. The overlayer thickness was determined from the Analyze results of the Fe 2p portion of the spectra. The model spectrum used for  $\gamma\text{-Fe}_2\text{O}_3$  was shifted upwards by 3.0 eV and the spectrum used for  $\text{Fe}_3\text{O}_4$  was shifted downwards by 0.5 eV for best fit.

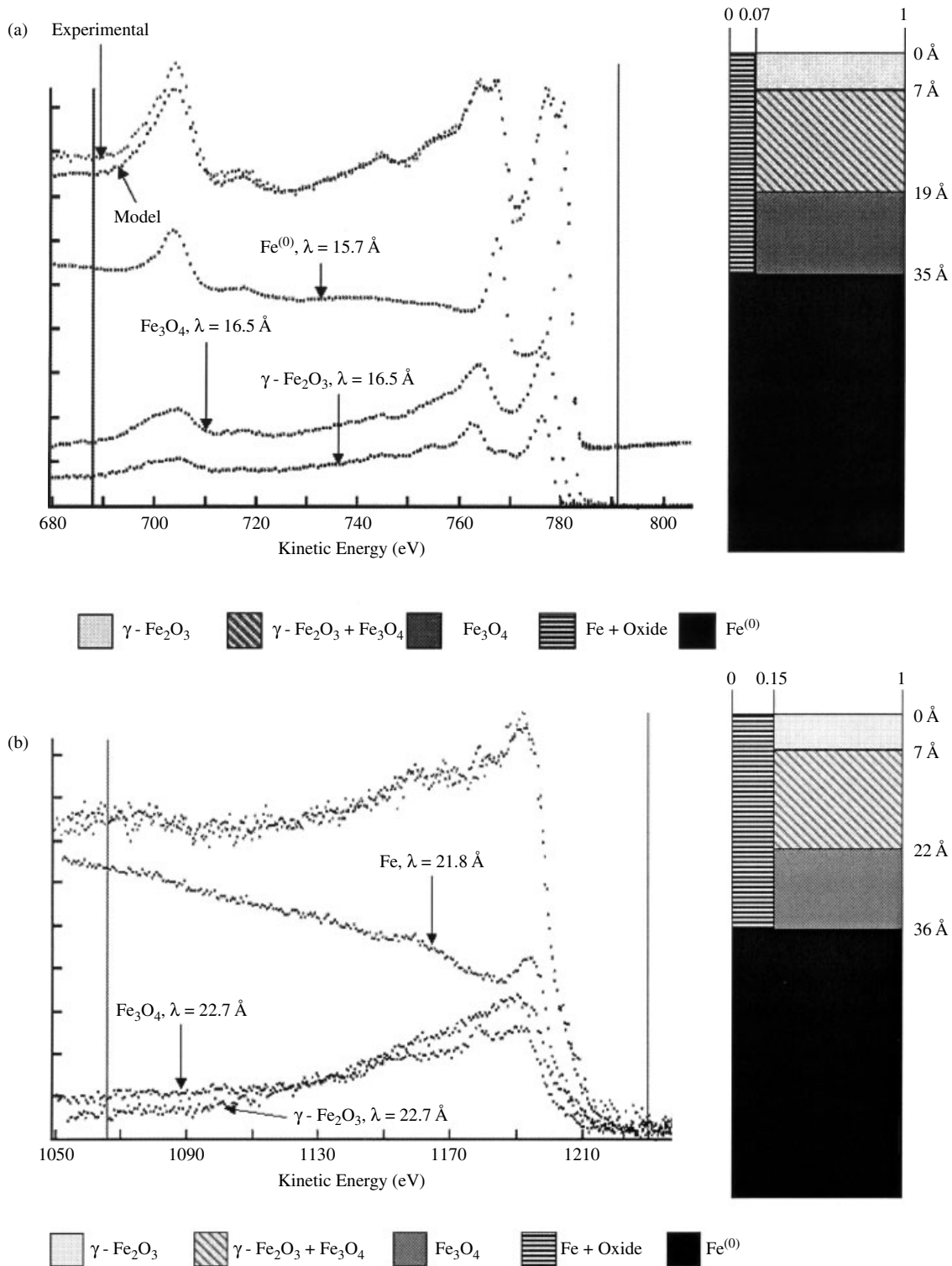


**Figure 6.** (a) The Fe 2p QUASES™ Generate results of 120 s air-exposed Fe surface analysed using an Al  $K\alpha$  x-ray source. The model spectrum used for  $\gamma\text{-Fe}_2\text{O}_3$  was shifted upwards by 2.5 eV to achieve the best fit. (b) The Fe 2s QUASES™ Generate results of 120 s air-exposed Fe surface analysed using a Zr L x-ray source. All three model spectra used were shifted to a lower kinetic energy by 0.5 eV to achieve the best fit. The model and experimental spectra overlap each other to a point where they are indistinguishable.

on an aluminium surface as part of an interlaboratory comparison of electron spectroscopic measurements.<sup>16</sup> For the same Fe oxide surface used in our studies, a value of  $2.25 \times 10^{16}$  atoms  $\text{cm}^{-2}$  was obtained. Subsequent re-analysis of the oxide layer thickness using QUASES™ Analyze showed no change in the thickness of the oxide layer.

Conversion of the graded oxide concentrations obtained by QUASES™ Generate and the calculated IMFP values gave an oxygen coverage of  $2.7 \times 10^{16}$  atoms  $\text{cm}^{-2}$ , which is ~20% greater than that obtained by NRA. This difference probably can be ascribed to an overestimation of the actual attenuation length by the IMFP used for the Fe 2p photoelectrons in the

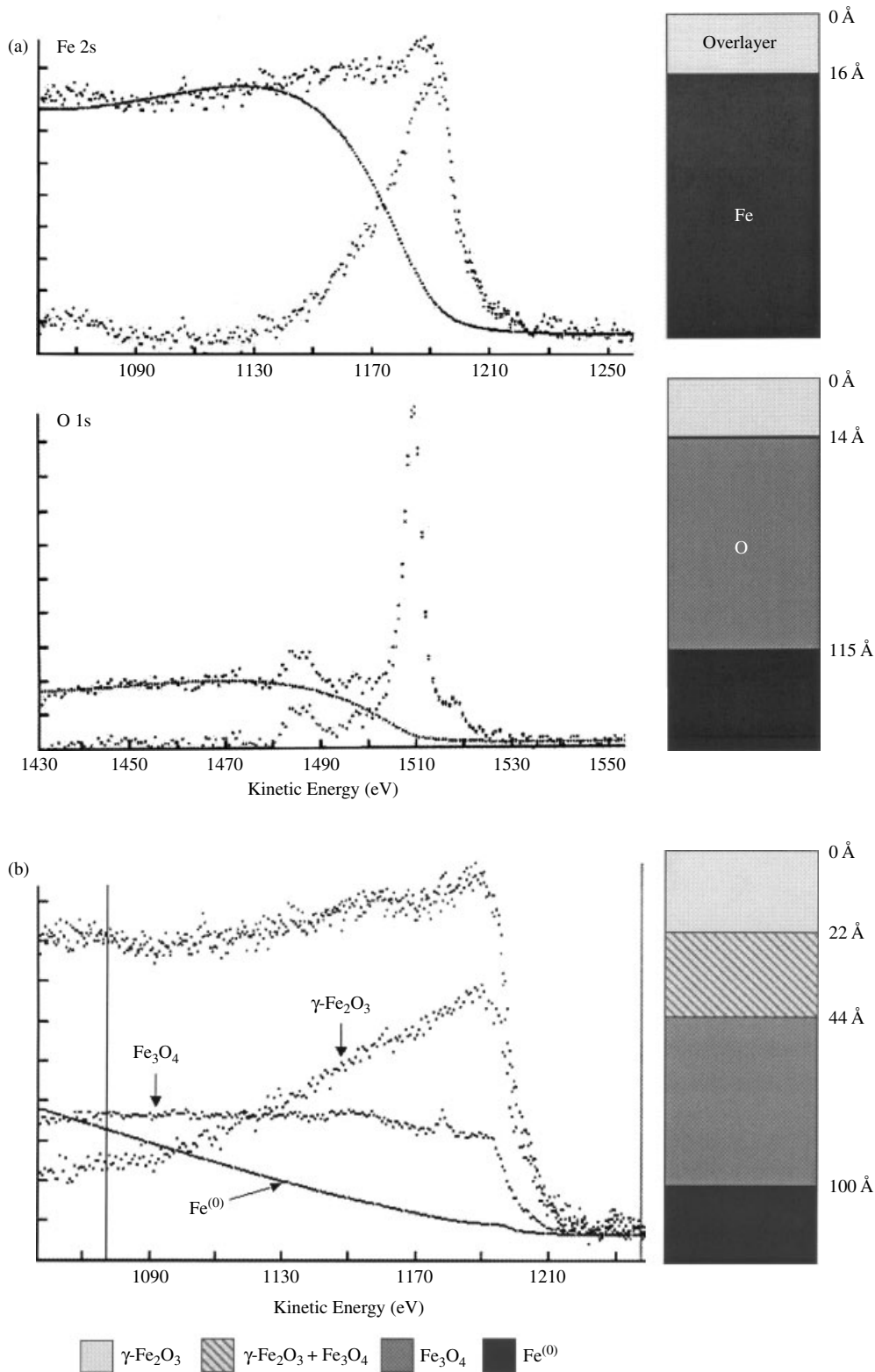


**Figure 7.** (a) The QUASES™ Analyze results for the Fe oxide film grown in air for 1 h at 150 °C, analysed using a Zr  $L\alpha$  x-ray source. (b) The Fe 2s QUASES™ Generate results for the Fe oxide film grown in air for 1 h at 150 °C, analysed using a Zr  $L\alpha$  x-ray source. The  $\gamma\text{-Fe}_2\text{O}_3$  and  $\text{Fe}_3\text{O}_4$  models were each shifted by 0.5 eV to a lower energy, whereas the Fe metal spectrum was shifted down by 1.0 eV to achieve the best fit. The model and experimental spectra overlap each other to a point where they are indistinguishable.

oxide matrix. The oxide thickness also was estimated using the Strohmeier equation,<sup>12</sup> which assumes a solid oxide layer and the same  $\lambda$  value for the oxide used in QUASES™. The resultant thickness calculated was 4.8 nm.

It should be noted that although the Generate results cannot account for the contaminate overlayer, its presence is obvious from the Analyze results. The effect of any contaminate overlayer in the Generate results is largely

annulled by the contaminate overlayers that were also present for all reference spectra.

To show how the model spectrum changes when other reference spectra are used,  $\alpha$ -Fe<sub>2</sub>O<sub>3</sub> was exchanged for  $\gamma$ -Fe<sub>2</sub>O<sub>3</sub> and the original spectrum was fitted again using Generate. The  $\alpha$  form could be considered to be a viable alternative because it is known to grow as an oxide layer on Fe surfaces when exposed to relatively high temperatures (250–550 °C).<sup>14a</sup> Figure 4 shows a comparison of both the  $\gamma$ - and  $\alpha$ -Fe<sub>2</sub>O<sub>3</sub> fit spectra to the experimental data for the first 70 eV kinetic energy range in the photoelectron spectrum. For both  $\gamma$ - and  $\alpha$ -Fe<sub>2</sub>O<sub>3</sub> analyses, similar surface oxide distributions were obtained. Visually, the  $\gamma$ -Fe<sub>2</sub>O<sub>3</sub> fit is significantly better in the top 50 eV compared with that for the  $\alpha$ -Fe<sub>2</sub>O<sub>3</sub> fit spectrum. In addition, statistical analysis of this portion of the fitted spectra gave an unnormalized  $\chi^2$  value of  $5.5 \times 10^6$  for the  $\gamma$ -Fe<sub>2</sub>O<sub>3</sub> fitted spectrum, which is significantly lower than the  $\chi^2$  value of  $1.4 \times 10^7$  for the  $\alpha$ -Fe<sub>2</sub>O<sub>3</sub> fitted spectrum.

Figure 5 indicates the results found after analysing the sample that was exposed to an oxygen pressure of  $1.3 \times 10^{-2}$  Pa for 2 min. The layer thickness was found to be lower than those obtained above with a mixed layer formed between  $\gamma$ -Fe<sub>2</sub>O<sub>3</sub>, Fe<sub>3</sub>O<sub>4</sub> and Fe metal. With the metal oxide interface found closer to the surface than for the oxide indicated in Fig. 3, the probability of Fe 2p electrons from the metal losing energy as they travel through the oxide is decreased. This observation can be seen as a decrease in slope of the Fe metal reference spectrum found in Fig. 5 compared with that found in Fig. 3. The difference in the presence of mixed oxide/metal layers between the air-exposed and  $1.3 \times 10^{-2}$  Pa exposed samples might indicate a difference in diffusion mechanism with a change in pressure and exposure time, an observation that could not be made using results from Analyze by itself, NRA or overlayer equations. These results emphasize the usefulness of QUASES™ Generate to model both thick and thin oxide films.

### Zirconium L $\alpha$ x-ray source

The applicability of QUASES™ methods to the same system of iron oxide films was also explored using a zirconium x-ray source. This achromatic x-ray source provided both Zr L $\alpha$  and L $\beta$  lines at 2042.4 and 2124.0 eV. Thus, the information depth for the Fe 2p line should be almost double that obtained with an Al K $\alpha$  source. X-ray photoelectron spectroscopy broad-scan spectra were acquired for an oxide film formed by 120 s air exposure of an Fe surface at room temperature after being vacuum annealed, first using monochromatic Al K $\alpha$  radiation and then immediately thereafter using achromatic Zr L radiation. The QUASES™ Analyze and Generate procedures could not be applied to the Fe 2p spectrum generated by the Zr L $\alpha$  line because of interference from the Zr L $\beta$ -generated Fe 2s and 2p lines. Consequently, the Zr L $\alpha$ -generated Fe 2s line was used for both QUASES™ procedures. Figure 6 compares the Generate results obtained using the Al and Zr sources. The oxide identifications and layer thicknesses for each oxide were strikingly similar for both sources, thus the use of the Zr source appears to be valid for these iron studies despite the broader photoelectron peaks produced by this

achromatic source. The chemical specificity of the extrinsic loss spectra does not appear to be degraded materially by the use of this source.

The increased information depth available from the Zr source was also demonstrated for an XPS study of an iron oxide layer substantially thicker than those studied above. Figure 7 shows the QUASES™ Analyze and Generate results for a vacuum-annealed iron oxide surface heated in air at 150 °C for 60 min. Both methods compute a total oxide thickness of  $10.0 \pm 0.1$  nm; an attempt to measure this same oxide thickness using the Al source and Generate did not allow for a well-fit model to be formed, therefore the Generate program seems to be limited to a thickness of  $\sim 5$ – $6\lambda$ ; such a limit still permits reliable data to be obtained with a Zr source but not with an Al source.

## CONCLUSIONS

The use of both QUASES™ programs allowed for a relatively accurate and detailed representation of the depth distribution of Fe oxide phases to be determined. The extrinsic loss structures were sufficiently characteristic of each specific Fe oxide species that it was much easier to use them for characterization purposes than the subtle differences<sup>17</sup> found in the Fe 2p core-line structures. Moreover, the time required to acquire such loss features was considerably shorter than is necessary for the core-line spectra. Comparison of the Generate results with those found using NRA suggested that the IMFP found using the TPP-2M equation was approximately 20% greater than the true attenuation length.

## REFERENCES

1. Tougaard S. *J. Va. Sci. Technol. A* 1990; **8**: 2197.
2. Tougaard S. *Surf. Interface Anal.* 1998; **26**: 249.
3. Tougaard S. *QUASES™, Version 4.4, Software for Quantitative XPS/AES of Surface Nano-Structures by Analysis of the Peak Shape and Background*, Quases Tougaard: Odense, 2000.
4. Tougaard S. *Solid State Commun.* 1987; **61**: 547.
5. Tougaard S. *User's Guide, QUASES: Quantitative Analysis of Surface by Electron Spectroscopy Version 4.4*, Quases Tougaard: Odense, 2000.
6. Jablonski A, Zemek J, Jiricek P. *Surf. Interface Anal.* 2001; **31**: 825.
7. Kover L, Tougaard S, Werner WSM, Cserny I. *Surf. Interface Anal.* 2002; **33**: 681.
8. Tougaard S, Hetterich W, Nielson AH, Hansen HS. *Vacuum* 1990; **41**: 1583.
9. Schleberger M, Fujita D, Scharfschwerdt C, Tougaard S. *Surf. Sci.* 1995; **331–333**: 942.
10. Moukassi M, Gougeon M, Steinmetz P, Dupre B, Gleitzer C. *Metall. Trans. B.* 1984; **15B**: 383.
11. Tanuma S, Powell CJ, Penn DR. *Surf. Interface Anal.* 1993; **21**: 165.
12. Strohmeier BR. *Surf. Interface Anal.* 1990; **15**: 51.
13. Shreir LL, Jarman RA, Burstein GT. *Corrosion Volume 1; Metal/Environment Reactions*. Butterworth Heinemann: Toronto, 1995; **7**: 21.
14. Cornell RM, Schwertmann U. *The Iron Oxides; Structure, Properties, Reactions, Occurrence and Uses*. VCH: New York, 1996; 452, 459.
15. Lin T, Seshadri G, Kelber J. *Appl. Surf. Sci.* 1997; **119**: 83.
16. Olefjor I, Mathieu HJ, Marcus P. *Surf. Interface Anal.* 1990; **15**: 681.
17. McIntyre NS, Zetaruk DG. *Anal. Chem.* 1977; **49**: 1521.